JACS
JOURNAL OF THE AMERICAN CHEMICAL SOCIETY

Subscriber access provided by American Chemical Society

Communication

Protein Backbone H−C and N−C Residual Dipolar and *J* Couplings: New Constraints for NMR Structure Determination

Keyang Ding, and Angela M. Gronenborn

J. Am. Chem. Soc., **2004**, 126 (20), 6232-6233• DOI: 10.1021/ja049049l • Publication Date (Web): 30 April 2004

Downloaded from http://pubs.acs.org on March 31, 2009

(A) $^{1}J_{N(i)CA(i)} = 8.6453-1.2129\cos(\psi_i)+2.8484\cos^2(\psi_i)$

(B)

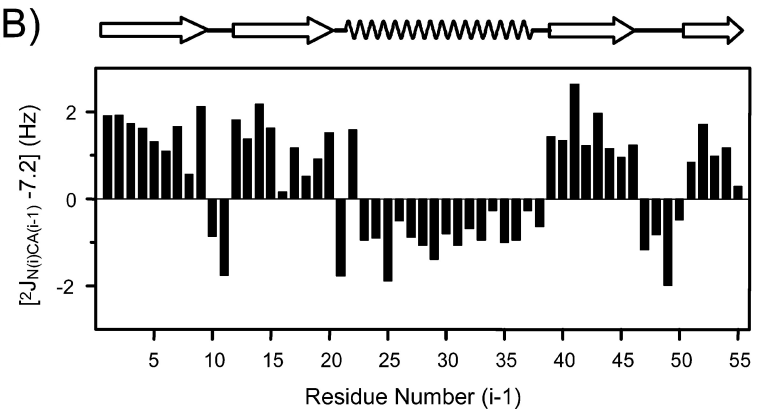

More About This Article

Additional resources and features associated with this article are available within the HTML version:

- Supporting Information
- Links to the 2 articles that cite this article, as of the time of this article download
- Access to high resolution figures
- Links to articles and content related to this article
- Copyright permission to reproduce figures and/or text from this article

View the Full Text HTML

ACS Publications
High quality. High impact.

Journal of the American Chemical Society is published by the American Chemical Society. 1155 Sixteenth Street N.W., Washington, DC 20036

J|A|C|S
COMMUNICATIONS

Published on Web 04/30/2004

Protein Backbone $^{1}H^{N}-^{13}C^{\alpha}$ and $^{15}N-^{13}C^{\alpha}$ Residual Dipolar and *J* Couplings: New Constraints for NMR Structure Determination

Keyang Ding and Angela M. Gronenborn*

Laboratory of Chemical Physics, National Institute of Diabetes and Digestive and Kidney Diseases, National Institutes of Health, Bethesda, Maryland 20892

Received February 19, 2004; E-mail: gronenborn@nih.gov

Backbone *J* couplings have a long history in NMR, notably ^{3}J couplings and their conformational dependences. Over the past decade, residual dipolar couplings (RDCs) in partially aligned proteins have also proven to be very important constraints for NMR structure determination.[1,2] One-bond and two-bond dipolar couplings such as $^{1}D_{NH}$, $^{2}D_{HCO}$, $^{1}D_{NCO}$, $^{1}D_{COCA}$, and $^{1}D_{CAHA}$ are frequently measured and used in the refinement of protein structures.[3] More recently, backbone $^{15}N-^{13}C^{\alpha}$ and $^{1}H^{N}-^{13}C^{\alpha}$ couplings have received more close attention.[4−9] For one-bond and two-bond $^{15}N-^{13}C^{\alpha}$ *J* couplings, a dependence on secondary structure was noted,[10] and a Karplus curve was parametrized for $^{2}J_{NCA(i-1)}$ with respect to ψ.[7] In this communication, we present an experiment that allows to very accurately measure $^{15}N-^{13}C^{\alpha}$ and $^{1}H^{N}-^{13}C^{\alpha}$ *J* as well as dipolar couplings in proteins. As evidenced by our data on protein GB1, a stringent relationship between $^{1}J_{NCA}$ and ψ exists, and we demonstrate that $^{2}J_{NCA(i-1)}$ can be used as a secondary structure index. In addition, the availability of accurate $^{1}D_{NCA}$, $^{2}D_{HCA}$, and $^{3}D_{HCA}$ dipolar couplings via this experiment yields yet another set of valuable constraints for NMR structure determination.

We employed our previously developed strategy[11,12] to design and implement a simple, sensitivity-enhanced experiment for measuring the $^{1}H^{N}-^{13}C^{\alpha}$ and $^{15}N-^{13}C^{\alpha}$ couplings. The pulse sequence of the experiment is depicted in Figure 1. In the period between a and b, either the anti-phase $2H_zN_y(i)C^{\alpha}_z(i-1)$ or the in-phase $H_zN_y(i)$ magnetization is created, depending on the location of the two 180° $^{13}C^{\alpha}$ pulses at the dashed-line open bar or solid-line open bars positions, respectively. Despite an additional intensity factor of $\sin(2\pi\Delta J_{CC})$ for the anti-phase magnetization $2H_zN_y(i)C^{\alpha}_z(i-1)$,[12] both in-phase and anti-phase magnetizations yield signals of equal intensity, given that $\sin(2\pi\Delta J_{CC}) \approx 1$. The pulse sequence after point b is the normal sensitivity-enhanced $^{15}N-^{1}H^{N}$ HSQC experiment,[13,14] with backbone $^{15}N-^{13}C^{\alpha}$ and $^{1}H^{N}-^{13}C^{\alpha}$ couplings active during the evolution and detection periods, respectively. The in-phase and the anti-phase datasets are acquired in an interleaved manner, and subsequent addition and subtraction of these two datasets result in two sensitivity-enhanced subspectra. Within each subspectrum, the $^{15}N-^{1}H^{N}$ cross-peaks exhibit an E.COSY doublet, passively split by the intraresidue $^{13}C^{\alpha}$ spin, and the corresponding E.COSY doublets in these two subspectra are displaced by the passive couplings of interresidue $^{13}C^{\alpha}$ spin.

Since $^{1}J_{NCA}$ ranges from 8.5 to 13.5 Hz, reasonably high digital resolution in the ^{15}N dimension is necessary for resolving the E.COSY doublet within each subspectrum. If partial overlap between the E.COSY doublets occurs, the one-bond $^{15}N-^{13}C^{\alpha}$ coupling cannot be correctly determined due to the displacement of the peak maxima.[15] Therefore, prerequistes for proteins consist of an apparent ^{15}N line-width of <8.5 Hz and making sure that high digital resolution in the ^{15}N dimension is employed. The latter is easy to achieve in the present experiment by using a large t_1(max), and any associated signal losses are compensated by implementing

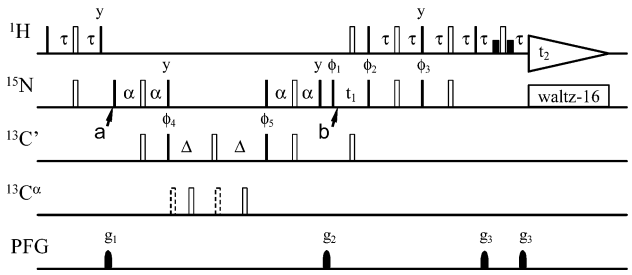

Figure 1. Pulse sequence for measuring backbone $^{1}H^{N}-^{13}C^{\alpha}$ and $^{15}N-^{13}C^{\alpha}$ couplings in proteins using sensitivity enhancement. Narrow (filled) and wide (open) bars represent 90° and 180° pulses with phase *x*, respectively, unless indicated otherwise. Proton 90° soft pulses of 1 ms duration are used for WATERGATE; they are indicated by short, filled bars. The carrier frequencies in the ^{1}H, ^{15}N, $^{13}C'$, and $^{13}C^{\alpha}$ channels are positioned at 4.7 ppm (water resonance), 118, 177, and 56 ppm, respectively. The power levels for the 90° and 180° pulses in the $^{13}C'$ and $^{13}C^{\alpha}$ channels are set at $\Delta\omega_0/(15)^{1/2}$ and $\Delta\omega_0/(3)^{1/2}$, respectively, with $\Delta\omega_0$ being the difference in Hz between the $^{13}C'$ and $^{13}C^{\alpha}$ carrier frequencies. The interpulse delays are $\tau = 2.5$ ms, $\alpha = 12.5$ ms, and $\Delta = 4.75$ ms. When the in-phase dataset collection is switched to the anti-phase one, the 180° pulses in the $^{13}C^{\alpha}$ channel are alternating from the positions of the open bars to those of the dashed bars. The phase cycles are as follows: $\phi_1 = 4(x, -x), 4(y, -y)$ for echo and $\phi_1 = 4(x, -x), 4(-y, y)$ for anti-echo; $\phi_2 = 4(x), 4(-x)$ and $\phi_3 = 4(y), 4(-y)$ for echo and $\phi_3 = 4(-y), 4(y)$ for anti-echo; $\phi_4 = x, x, -x, -x$ and $\phi_5 = x$ for the in-phase dataset and $\phi_5 = y$ for the anti-phase dataset; $\phi_{Rec} = x, -x, -x, x, -x, x, x, -x, -y, y, y, -y, y, -y, -y, y$. The PFG g_1, g_2, and g_3 are sine-shaped with maximal 20 G/cm and durations of 3, 1.5, and 0.6 ms, respectively.

the sensitivity enhancement. For small, compact proteins such as GB1,[16] the apparent ^{15}N line-widths range from 6 to 8 Hz, and measuring an accurate data set for GB1 is therefore easily possible. This allows one to obtain an excellent parametrization of the Karplus-curve for both one-bond and two-bond $^{15}N-^{13}C^{\alpha}$ *J* couplings.

Residual dipolar couplings were measured for GB1 aligned in PF1 phage. All experimental $^{1}D_{NCA}$, $^{2}D_{HCA}$, $^{3}D_{HCA}$, and $^{2}D_{NCA}$ couplings are in very good agreement with predicted[17] values, calculations based on the refined NMR structure[18] (PDB code: 3GB1) as the model with alignment tensor parameters, $D_a = 6.836$ and $R = 0.637$. The correlation coefficients are 0.976, 0.983, 0.944, and 0.833 for $^{2}D_{HCA}$, $^{1}D_{NCA}$, $^{3}D_{HCA}$, and $^{2}D_{NCA}$, respectively (the $^{2}D_{HCA}$, $^{1}D_{NCA}$, and $^{3}D_{HCA}$ correlations are supplied in Figure S1). The magnitudes of $^{2}D_{HCA}$ and $^{1}D_{NCA}$ are comparable to those of $^{2}D_{HCO}$ and $^{1}D_{NCO}$ and that of $^{3}D_{HCA}$ is comparable to those of $^{1}D_{NCA}$ and $^{1}D_{NCO}$.[11] Even for the very small (<0.3 Hz) $^{2}D_{NCA}$ couplings (Figure 2A), a good correlation between the measured and predicted values is obtained, demonstrating the reliability and robustness of the present experiment for extracting accurate values. Indeed, we observe a significantly better agreement between measured and predicted values than previously reported,[9] either due to the superior accuracy achieved in our experiment or the use of an incorrect model structure in the previous report.

10.1021/ja049049l **Not subject to U.S. copyright. Publ. 2004 Am. Chem. Soc.**

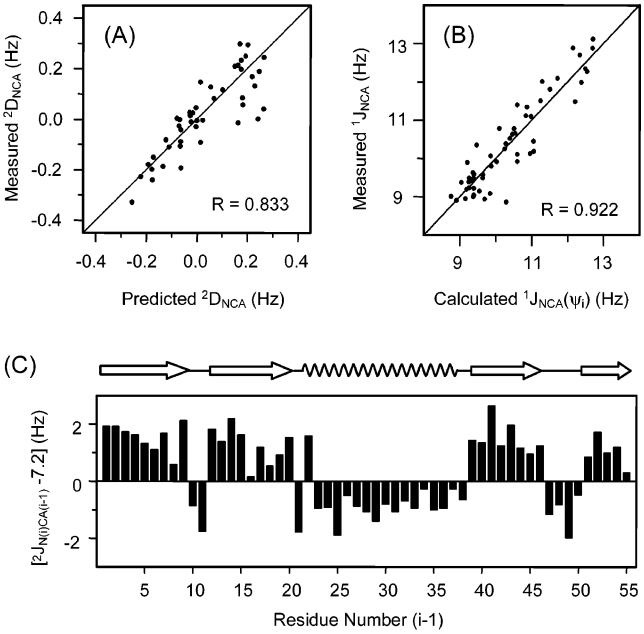

Figure 2. Correlation between measured and predicted $^2D_{NCA}$ residual dipolar couplings (A) and $^1J_{NCA}$ (B) for protein GB1. In (A), calculated values were obtained based on the refined NMR structure (PDB code: 3GB1) using the alignment tensor parameters $D_a = 6.836$ and $R = 0.637$. In (B), calculated values were obtained using the Karplus equation $^1J_{N(i)CA(i)} = 8.6453 - 1.2129\cos[\psi(i)] + 2.8484\cos^2[\psi(i)]$ with backbone dihedral angles ψ extracted from the refined NMR structure (PDB code: 3GB1). (C) Normalized values of $^2J_{NCA(i-1)}$ $[^2J_{NCA(i-1)} - 7.2]$ versus residue number $(i - 1)$. The close correspondence between secondary structure elements (top) and positive (β-strand) and negative deviations (α-helix and -turns) is apparent. For the determination of the residual dipolar couplings, GB1 was aligned in a suspension of 15 mg/mL PF1 in 95%H_2O/5%D_2O, pH 7. The protein concentration was ∼0.5 mM. Each spectrum was accumulated with 16 scans and took about 12 h total measuring time. A digital resolution of 2.44 Hz per time domain point and $t_1(\max) = 204.8$ ms were used for the present measurements. Except for two resides, Q2 and T55, that exhibit partially overlapped resonances in the alignment medium, complete sets of dipolar couplings were obtained.

Figure 2B displays the correlation (correlation coefficient: 0.922) between the measured and calculated $^1J_{NCA}$ for protein GB1 based on the Karplus relationship $J = A + B\cos(\psi) + C\cos^2(\psi)$. Least-squares fit of the experimentally determined couplings with respect to the torsion angle ψ yields

$$^1J_{NCA(i)} = 8.6453 - 1.2129\cos[\psi(i)] + 2.8484\cos^2[\psi(i)] \quad (1)$$

for $^1J_{NCA}$. The dihedral angles ψ were extracted from the refined NMR structure (PDB code: 3GB1).[18] A slightly better correlation was observed for $^1J_{NCA}$ than for $^2J_{NCA(i-1)}$, different from a previous report.[7] For $^2J_{NCA(i-1)}$, a striking feature in the correlation diagram is the clustering of data points into two distinct regions associated with α-helical and turn residues and β-sheet residues, respectively (Figure S2). With the exception of only one data point, namely ($^2J_{N(9)CA(8)}$, ψ_8), all other $^2J_{NCA(i-1)}$ values reside in regions corresponding to their secondary structure. This characteristic suggests that $^2J_{NCA}$ values can be used to assign secondary structure propensity similar to methods using traditional $^3J_{HNHA}$ coupling constants.[19] As shown in Figure 2C, a plot of the normalized coupling $[^2J_{NCA(i-1)} - 7.2]$ against residue number $(i - 1)$ allows easy delineation of secondary structure elements. Note that the value of 7.2 Hz used here basically divides the clusters of couplings in α-helical and -turn regions from those in β-strands (see Figure S2), which is quite close to the average value of 7.5 Hz obtained by averaging the equation $^2J_{N(i)CA(i-1)} = 7.8509 - 1.5176\cos[\psi(i-1)] - 0.6616\cos^2[\psi(i-1)]$ over the ψ angle. Therefore, the two-bond $^2J_{NCA}$ couplings can be used as a secondary structure index and the one-bond $^1J_{NCA}$ couplings can be employed via the parametrized Karplus eq 1 in NMR structure refinement.

In conclusion, we devised a simple, sensitivity-enhanced experiment for accurate measurement of backbone $^{15}N-^{13}C^\alpha$ and $^1H^N-^{13}C^\alpha$ couplings in proteins. This method will only work well for small, folded proteins (<10 kDa) or others with apparent ^{15}N line-widths <8.5 Hz. For GB1 the experimentally determined $^2D_{HCA}$, $^1D_{NCA}$, $^3D_{HCA}$, and $^2D_{NCA}$ residual dipolar couplings agree well with theoretical values calculated on the basis of the refined NMR structure[18] (PDB code: 3GB1). The one-bond $^1J_{NCA}$ couplings display good Karplus-type dependence on the backbone dihedral ψ angles, and two-bond $^2J_{NCA}$ couplings allow derivation of a secondary structure index. Therefore, both residual dipolar and J couplings measured in the above manner provide useful constraints for protein NMR structure refinement.

Acknowledgment. This work was supported in part by the Intramural AIDS Targeted Antiviral Program of the Office of the Director of the National Institutes of Health (A.M.G.).

Supporting Information Available: All experimentally measured $^2J_{HCA}$, $^1J_{NCA}$, $^3J_{HCA}$, and $^2J_{NCA}$ values for GB1(Table S1); correlations between measured and predicted residual dipolar couplings $^1D_{NCA}$, $^2D_{HCA}$, and $^3D_{HCA}$ (Figure S1); relation between measured and calculated $^2J_{NCA}$ couplings for GB1 using the equation $^2J_{N(i)CA(i-1)} = 7.8509 - 1.5176\cos[\psi(i-1)] - 0.6616\cos^2[\psi(i-1)]$ (Figure S2); two experimental subspectra (A) and (B) and splitting patterns and extraction of coupling values indicated in the expanded spectra (C) and (D) (Figure S3). This material is available free of charge via the Internet at http://pubs.acs.org.

References

(1) Tolman, J. R.; Flanagan, J. M.; Kennedy, M. A.; Prestegard, J. H. *Proc. Natl. Acad. Sci. U.S.A.* **1995**, *92*, 9279−9283.
(2) Tjandra, N.; Bax, A. *Science* **1997**, *278*, 1111−1114.
(3) deAlba, E.; Tjandra, N. *Prog. Nucl. Magn. Reson. Spectrosc.* **2002**, *40*, 175−197.
(4) Permi, P.; Annila, A. *J. Biomol. NMR* **2000**, *16*, 221−227.
(5) Permi, P.; Rosevear, P. R.; Annila, A. *J. Biomol. NMR* **200**, *17*, 43−54.
(6) Heikkinenen, S.; Permi, P.; Kilpelaenen, I. *J. Magn. Reson.* **2001**, *148*, 53−60.
(7) Wirmer, J.; Schwalbe, H. *J. Biomol. NMR* **2002**, *23*, 47−55.
(8) Bhavesh, N. S.; Chatterjee, A.; Panchal, S. C.; Hosur, R. V. *Biochem. Biophys. Res. Commun.* **2003**, *311*, 678−684.
(9) Wienk, H. L. J.; Martinez, M. M.; Yalloway, G. N.; Schmidt, J. M.; Perez, C.; Ruterjans, H.; Lohr, F. *J. Biomol. NMR* **2003**, *25*, 133−145.
(10) Delaglio, F.; Torchia, D. T.; Bax, A. *J. Biomol. NMR* **1991**, *1*, 439−446.
(11) Ding, K.; Gronenborn, A. M. *J. Magn. Reson.* **2002**, *158*, 173−177.
(12) Ding, K.; Gronenborn, A. M. *J. Magn. Reson.* **2004**, *167*, 253−258.
(13) Palmer, A. G., III; Cavanagh, J.; Wright, P. E.; Rance, M. *J. Magn. Reson.* **1991**, *93*, 151−170.
(14) Cavanagh, J.; Palmer, A. G., III; Wright, P. E.; Rance, M. *J. Magn. Reson.* **1991**, *91*, 429−436.
(15) Neuhaus, D.; Wagner, G.; Vasak, M.; Kaegi, J. H. R.; Wuthrich, K. *Eur. J. Biochem.* **1985**, *151*, 257−273.
(16) Gronenborn, A. M.; Filpula, D. R.; Essig, N. Z.; Achari, A.; Whitlow, M.; Wingfield, P. T.; Clore, G. M. *Science* **1991**, *253*, 657−661.
(17) Zweckstetter, M.; Bax, A. *J. Am. Chem. Soc.* **2000**, *122*, 3791−3792.
(18) Kuszewski, J.; Gronenborn, A. M.; Clore, G. M. *J. Am. Chem. Soc.* **1999**, *121*, 2337−2338.
(19) Pardi, A.; Billeter, M.; Wuthrich, K. *J. Mol. Biol.* **1984**, *180*, 741−751.

JA049049L